



OPEN ACCESS

EDITED BY

Xiao Ouyang,
Hunan University of Finance and
Economics, China

REVIEWED BY

Wei Liao,
Hunan University of Finance and
Economics, China
Shaohua Zhao,
Ministry of Ecology and Environment
Center for Satellite Application on
Ecology and Environment, China

*CORRESPONDENCE

Guanghui Tian,
✉ tianguanghui@xcu.edu.cn

RECEIVED 25 June 2023

ACCEPTED 14 August 2023

PUBLISHED 25 August 2023

CITATION

Meng F, Yan S, Tian G and Wang Y (2023),
Surface urban heat island effect and its
spatiotemporal dynamics in metropolitan
area: a case study in the Zhengzhou
metropolitan area, China.
Front. Environ. Sci. 11:1247046.
doi: 10.3389/fenvs.2023.1247046

COPYRIGHT

© 2023 Meng, Yan, Tian and Wang. This is
an open-access article distributed under
the terms of the [Creative Commons
Attribution License \(CC BY\)](https://creativecommons.org/licenses/by/4.0/). The use,
distribution or reproduction in other
forums is permitted, provided the original
author(s) and the copyright owner(s) are
credited and that the original publication
in this journal is cited, in accordance with
accepted academic practice. No use,
distribution or reproduction is permitted
which does not comply with these terms.

Surface urban heat island effect and its spatiotemporal dynamics in metropolitan area: a case study in the Zhengzhou metropolitan area, China

Fei Meng¹, Shuling Yan¹, Guanghui Tian^{2*} and Yudong Wang³

¹School of Foreign Languages and Tourism, Henan Institute of Economics and Trade, Zhengzhou, China, ²College of Urban and Environmental Sciences, Xuchang University, Xuchang, China, ³Key Research Institute of Yellow River Civilization and Sustainable Development and Collaborative Innovation Center on Yellow River Civilization, Henan University, Kaifeng, China

The deterioration of the urban surface thermal environment has seriously affected regional environments and human health, becoming a critical ecological problem faced by cities worldwide. This study focused on surface urban heat island effect in metropolitan area and selected the emerging metropolitan area of Zhengzhou, China, as a case study. Based on the MODIS land surface temperature data obtained from the Google Earth Engine the surface urban heat island intensity (SUHII) was calculated and its temporal and spatial dynamics were analyzed from 2003 to 2022. The main findings indicated that Zhengzhou, the core city of the metropolitan area, had the strongest urban heat island effect with day surface urban heat island intensity of 1.10°C and night SUHII of 1.39°C. Generally, the average annual SUHII was higher during the day than at night, and the maximum value was detected in summer (2.43°C). SUHII showed an increasing trend at night, especially in summer during the study period. It decreased obviously in urban centers during the day, while it increased obviously in the outer urban areas at night. The results of this study contributed to the understanding of the spatiotemporal dynamics of the urban heat island effect in the Zhengzhou metropolitan area.

KEYWORDS

urban heat island effect, surface heat island intensity, trend analysis, spatial disparities, GEE

1 Introduction

The urban heat island effect is defined as the phenomenon by which temperatures in urban areas are higher than those in surrounding rural areas. This effect can have an impact on the microclimate, atmospheric environment, and the wellbeing and health of urban residents (Manoli et al., 2019; Yang D. et al., 2022; Vinayak et al., 2022; Ma and Dong, 2023). Within the context of global climate change, urban heat islands exacerbate the risk of heat-related deaths (Wang J. et al., 2021; Tong et al., 2021). With the acceleration of urbanization, the urban heat island effect has become an important environmental issue. The phenomenon is caused by the gradual replacement of natural land surfaces (vegetation and water bodies) with impermeable surfaces and by the increase in heat emissions derived from urban human activities. As China's massive urbanization continues to progress, the expansion of urban

land use and population growth will continue to have a significant impact on the urban heat island effect (Chen et al., 2018; Vinayak et al., 2022). Studying urban heat islands can provide a theoretical basis for urban planning and sustainable development, which is urgently needed and have significant practical implications for improving the living environment of urban residents.

Extensive research has already been conducted on the urban heat island effect. In terms of measurement methods, it is common to calculate the air temperature or land surface temperature differences between urban and suburban areas based on data obtained on-site or using remote sensing technology (Khan and Chatterjee, 2016; Levermore et al., 2018; Zhang X. et al., 2022). In recent years, the urban heat island effect has been increasingly and primarily quantified by calculating the surface urban heat island intensity (SUHII) using land surface temperature data derived from remote sensing (Deilami et al., 2018; Kumar and Mishra, 2019; Yao et al., 2019). The temporal and spatial characteristics of SUHII and its influencing factors are the main focus of current research. Typically, Meng et al. (2018) conducted a temporal analysis of the urban heat island effect in Beijing and found a higher average daytime SUHII, which was associated with higher density of impervious surfaces (Meng et al., 2018). Wang et al. (2021) investigated urban heat island and the influences of air pollutants in cities in the Yangtze River Delta during 2015–2019 and also documented that annual average daytime SUHII was higher than nighttime SUHII, and O₃ concentration presented a significant positive correlation with daytime SUHII (Wang Y. et al., 2021). Zhang et al. (2022) documented a decrease in SUHII in the Yangtze River Delta, Beijing-Tianjin-Hebei region, and the middle reaches of the Yangtze River from 2003 to 2019, as well as an increase in SUHII in the Chengdu-Chongqing and Pearl River Delta urban agglomerations, with significant impacts of land cover changes on the urban heat island effect in the Beijing-Tianjin-Hebei, Yangtze River Delta, and Chengdu-Chongqing urban agglomerations (Zhang H. et al., 2022). Additionally, Siddiqui et al. (2021) investigated the temporal variations of SUHII in three cities in India from 2001 to 2019, revealing a significant increasing trend in annual average SUHII in Kolkata and Pune, with particularly high warming rates during summer, especially at night. (Siddiqui et al., 2021). Generally, previous studies have mainly shown that the urban heat island effect is obvious in summer and at night. Aspects of the underlying surface, including land use/cover, urban morphology, landscape pattern, as well as anthropogenic heat and atmospheric pollution, are considered to be major factors influencing the urban heat island effect (Wang et al., 2018; Li et al., 2020; Wang J. et al., 2021; Yang F. et al., 2022; Sun et al., 2022). Regional climate conditions also have an important impact on the urban heat island effect. For example, Wu et al. (2019) explored the heat islands of 44 cities in South America based on the Köppen-Geiger climate zones and found that the average SUHII in all climate zones (except for arid zones) was higher during the day than at night (Wu et al., 2019).

In China, research is concerned with this issue in multiple cities or at the national scale (Peng et al., 2012; Debbage and Shepherd, 2015; Zhao et al., 2016; Yang et al., 2019; Liu Y. et al., 2020; Ke et al., 2021; Marando et al., 2022), especially where major megacities are located, such as the Yangtze River Delta region and the Beijing-Tianjin-Hebei region (Zhao et al., 2016; Liu X. et al., 2020; Zhang X.

et al., 2022). These studies have greatly contributed to understanding this harmful phenomenon and the mechanisms that influence it. While, urban heat island effects may have different temporal and spatial characteristics in different regions and at different stages of urban expansion. Particularly, with the development of urban agglomerations, the urban heat island effect may extend beyond individual cities and spread throughout the entire urban agglomeration. While there have been numerous studies on the urban heat island effect in single cities or megacities, research specifically focusing on urban agglomerations remains relatively limited. Previous studies have mainly examined the temporal variations of the overall urban heat island effect in single cities and the differences among different cities (Meng et al., 2018; Yang et al., 2019). Some scholars have also investigated the spatial differences of the urban heat island effect within urban areas, such as the differences among different urban functional zones (Zhao et al., 2016; Ke et al., 2021). However, less attention has been given the temporal trends of the urban heat island effect within urban areas and its spatial differences. Therefore, further investigation is warranted to explore these aspects.

Therefore, to bridge this knowledge gap, long-term MODIS land surface temperature data obtained from the Google Earth Engine (GEE) cloud platform and related auxiliary data were here used to measure the SUHII of each city in the Zhengzhou metropolitan area from 2003 to 2022. Then, the annual variation and seasonal differences in SUHII during the day and at night were analyzed. Finally, the temporal trends of this parameter and its spatial differences within the cities in the area were further explored. The aim was to describe the spatiotemporal dynamics of the urban heat island effect and provide support for the formulation of policies to mitigate this harmful phenomenon in the Zhengzhou metropolitan area.

2 Materials and methods

2.1 Study area

The Zhengzhou metropolitan area is located in the central and lower reaches of the Yellow River in China, a favorable geographical location at the center of China (Figure 1). Its total area is about 15.90 thousand square kilometers. It consists of five cities, i.e., Zhengzhou, Kaifeng, Xuchang, Xinxiang, and Jiaozuo, among which Zhengzhou is one of the nine national central cities of China. The Zhengzhou metropolitan area is characterized by a mainly flat terrain and mild climate. It is a key development area in Henan Province, and its economic hinterland is vast and has a great potential for future expansion. In 2021, the permanent population in the Zhengzhou metropolitan area was 31.60 million people, accounting for 32% of the total population in Henan Province; the regional gross domestic product was 2.43 trillion RMB, accounting for 41% of that of Henan Province (Henan Province Bureau of Statistics, 2022). It is one of the most developed and fastest-growing regions in central and western China. However, the rapid expansion of cities has damaged the urban ecological environment, leading to changes in the thermal environment and to the consequent urban heat island effect in this region.

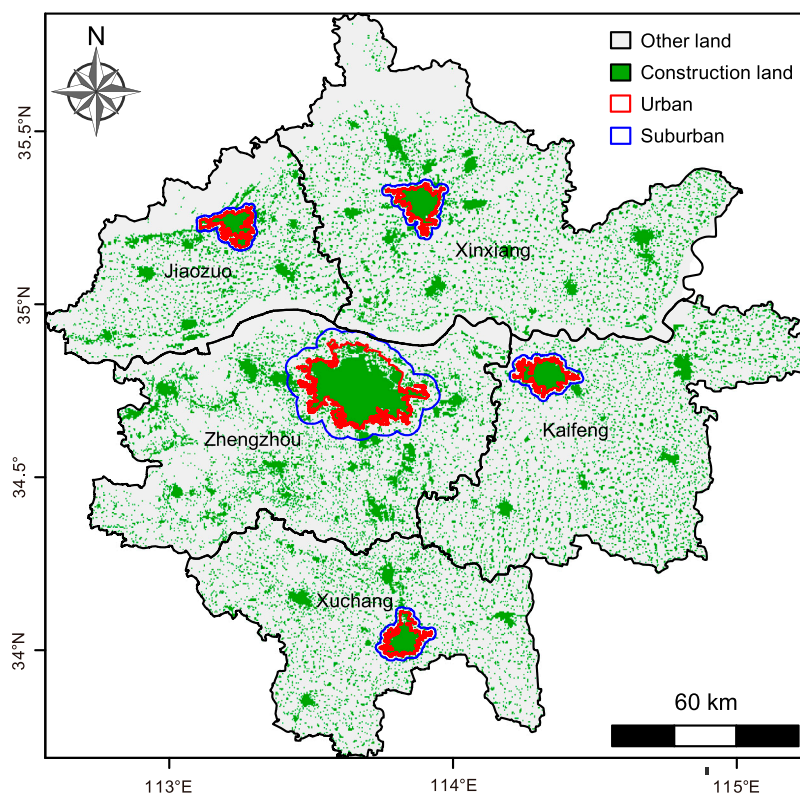


FIGURE 1
Map of the Zhengzhou metropolitan area and its urban and suburban areas.

2.2 Data sources and preprocessing

2.2.1 Surface temperature data

In previous studies, surface temperature has been used as a common indicator to quantify the urban heat island effect (Schwarz et al., 2011; Halder et al., 2021; Sekertekin and Zadbagher, 2021). In this study, the MODIS surface temperature product dataset, MYD11A2 V6.1, was obtained from the NASA's Land Processes Distributed Active Archive Center (LP DAAC, <https://lpdaac.usgs.gov>) through the GEE platform. This dataset has a spatial resolution of 1 km and provides daytime and nighttime surface temperatures over an average period of 8 days. The images in the form of average values were synthesized to obtain the 20-year, annual, and seasonal land surface temperatures for the Zhengzhou metropolitan area on the GEE. Seasons were defined based on the traditional Chinese classification: spring (from March to May), summer (from June to August), autumn (from September to November), and winter (from December to February of the following year). The MYD11A2 dataset is available from 4 July 2002, therefore data from 1 March 2003, to 28 February 2023, were used in the present investigation.

2.2.2 Land use data

Land use data were obtained from the China National Land Use/Cover Change dataset at the Resource and Environment Science and Data Center (<https://www.resdc.cn/>). This dataset is a national-scale thematic database of variations in land use/cover in China that was compiled through manual visual interpretation of Landsat-derived

remote sensing images. The dataset, which has been updated to 2020, adopts a two-level classification system, with Level 1 consisting of six categories: cultivated land, forest land, grassland, water area, construction land, and unused land; the spatial resolution is 30 m.

2.3 Methods

2.3.1 Subdivision of urban and suburban areas

A core issue in the remote sensing-based monitoring of urban heat islands is how to subdivide urban and suburban areas. In this study, an area buffer method was developed to determine the boundary between urban and suburban areas based on relevant previous investigations (Clinton and Gong, 2013; Zhou et al., 2014; Tan and Li, 2015; Liu X. et al., 2020). This method consisted of four steps. Firstly, land use data were processed using a binary system; construction land was defined as 1 and other land cover types were defined as 0. Secondly, the largest urban patches were identified and selected, and a 3×3 convolution filter was applied to extract urban boundaries. Thirdly, the "holes" formed by non-urban land cover within the urban boundary were filled to obtain a complete urban boundary. The resolution was very high: some patches north and east of Zhengzhou are separated from urban Zhengzhou by the Jialu River, Lian-Huo highway, and their green belt. In reality, these patches are also part of Zhengzhou's urban area (they are main areas of Huiji District and Zhengdong New District). Thus, mask processing was applied to gap areas north and east of

Zhengzhou. Finally, equal-area buffers were established outside the urban boundary to determine the suburban area (Liao et al., 2021). The derived urban and suburban boundaries are shown in Figure 1. The method ensures that urban built-up areas are concentrated contiguous areas, and the urban area is similar to the outer area, which is conducive to the comparison of surface temperature in the two regions.

2.3.2 Surface urban heat island intensity

SUHII is commonly measured by calculating the differences in surface temperature between urban area or sites and suburban area or sites. Based on the above-mentioned preprocessing of daytime and nighttime surface temperature data at the interannual and seasonal scales, we calculated the difference in the average surface temperature of all pixels between the urban and suburban areas of each city and considered it as the surface heat island intensity of each city. The following equation was applied:

$$SUHII = \frac{\sum_{u=1}^n T_u}{n} - \frac{\sum_{s=1}^m T_s}{m}$$

where *SUHII* is the surface urban heat island intensity, *n* and *m* represent the total number of pixels in urban and suburban areas, respectively. *T_u* is the surface temperature in pixel *u* in urban areas, and *T_s* is the surface temperature in pixel *s* in suburban areas.

2.3.3 Sen's slope

Sen's slope, also known as Theil-Sen median, is a robust nonparametric statistical method used to calculate trends. As it has a high computational efficiency and is insensitive to measurement errors and outliers, this method is commonly used in trend analyses of long time series data. It is described by the following equation:

$$\beta = \text{mean}\left(\frac{x_j - x_i}{j - i}\right), (j > i)$$

where, *x_i* and *x_j* are the time series of observed values (surface temperature in the current study). A *β* value higher than 0 indicates an upward trend in the time series, while a *β* value lower than 0 indicates a downward trend.

The Sen's slope method is usually applied in combination with the Mann-Kendall test.

2.3.4 Mann-Kendall test

The Mann-Kendall test is a nonparametric statistical method. Its null hypothesis assumes the absence of a trend, while the alternative hypothesis assumes the existence of some trend. Through this test, the difference between each data point and all subsequent data points in a given time series was calculated, and the trend of the time series was then determined based on the sign of the differences obtained. Finally, by applying the rank-sum test it was established whether the trend was significant or not. A significant test result indicated the presence of a trend in the time series; otherwise, it was concluded that there was no trend.

The test was described as follows:

The standardized test statistic *Z* for time series *X_i*, *i* = 1, 2, ..., *i*, ..., *j*, ..., *n*, is defined as:

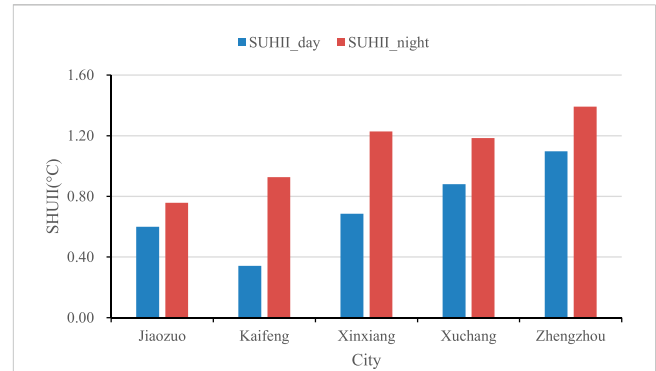


FIGURE 2
Average daytime and nighttime surface heat island intensity in each city of the Zhengzhou metropolitan area.

$$Z = \begin{cases} \frac{S}{\sqrt{\text{VAR}(S)}} & (S > 0) \\ 0 & (S = 0) \\ \frac{S + 1}{\sqrt{\text{VAR}(S)}} & (S < 0) \end{cases}$$

$$S = \sum_{i=1}^{n-1} \sum_{j=i+1}^n \text{sign}(x_j - x_i)$$

$$\text{sign}(\theta) = \begin{cases} 1 & (\theta > 0) \\ 0 & (\theta = 0) \\ -1 & (\theta < 0) \end{cases}$$

where, *x_i* and *x_j* are the time series, and *n* is the time series length. If *n* ≥ 8, the expectation and variance of *S* is:

$$E(S) = 0$$

$$\text{VAR}(S) = \frac{n(n-1)(2n+5)}{18}$$

If $|Z| > Z_{1-\frac{\alpha}{2}}$ (*α* is the given significance level), the time series exhibits a significant variation trend. When *α* is 0.05, *Z* = 1.96. If $|Z| > 1.96$, the variation trend is significant at the confidence level of 95%.

3 Results

3.1 Daytime and nighttime SUHII in each city of the Zhengzhou metropolitan area

3.1.1 Average daytime and nighttime SUHII in each city

Based on the daytime and nighttime land surface temperature data from 2003 to 2022, the multi-year average land surface temperatures of urban and suburban areas and the annual average SUHII of each city during the day and at night were calculated and are shown in Figure 2. Among the cities in the Zhengzhou metropolitan area, Zhengzhou showed the strongest SUHII during the day (1.10°C) and at night (1.39°C). The annual average SUHII during the day in the other cities were all less than 1°C. However, at night, Xinxiang and Xuchang exhibited SUHII higher than 1°C, reaching 1.23°C and 1.18°C, respectively. The lowest annual average SUHII

TABLE 1 Surface heat island intensity in each city of the Zhengzhou metropolitan area across seasons.

City	Day				Night			
	Spring	Summer	Autumn	Winter	Spring	Summer	Autumn	Winter
Jiaozuo	1.04	1.53	0.34	-0.54	0.94	0.95	0.77	0.71
Kaifeng	0.67	1.89	0.26	-0.70	1.12	0.90	1.10	1.14
Xinxiang	2.05	1.78	0.06	-0.72	1.46	1.27	1.27	1.38
Xuchang	2.11	1.68	0.35	-0.26	1.57	1.19	1.28	1.33
Zhengzhou	1.36	2.43	0.78	-0.28	1.47	1.35	1.40	1.67
Mean	1.44	1.86	0.36	-0.50	1.31	1.13	1.16	1.25

during the day was 0.34°C, detected in Kaifeng, while the lowest value at night was 0.76°C, detected in Jiaozuo. Overall, the multi-year average land surface temperatures of urban and suburban areas in the Zhengzhou metropolitan area during the day were 26.38°C and 25.66°C, respectively, while at night they were 10.34°C, and 9.24°C, respectively. The SUHII in the Zhengzhou metropolitan area was higher at night (1.10°C) than during the day (0.72°C).

3.1.2 Daytime and nighttime SUHIs in different seasons in each city

Subsequently, the average daytime and nighttime SUHIs in each city in different seasons were calculated, and the results are shown in Table 1. The highest daytime SUHII was detected in Xuchang in spring (2.11°C), followed by that in Xinxiang (2.05°C), while that in Kaifeng was the lowest (0.67°C). In summer, the highest SUHII was detected in Zhengzhou, where it reached 2.43°C, while the values in other cities were all below 2.00°C. In autumn, the SUHII in Zhengzhou was still the highest, reaching 0.78°C, while that in Xinxiang was the lowest, at only 0.06°C. In winter, the SUHIs in all cities were negative due to the cold island effect. The strongest and weakest effects were detected in Xinxiang (-0.72°C) and Zhengzhou (-0.28°C), respectively.

At night, the highest SUHII was recorded in Xuchang in spring (1.57°C), followed by the values in Zhengzhou (1.47°C) and Xinxiang (1.46°C). The lowest SUHII in spring was detected in Kaifeng (0.94°C). In summer, Zhengzhou exhibited the highest SUHII (1.35°C), followed by Xinxiang (1.27°C) and Xuchang (1.19°C), while the lowest value was detected in Kaifeng (0.90°C). In autumn, the highest SUHII was still recorded in Zhengzhou (1.40°C), followed by Xuchang (1.28°C) and Xinxiang (1.27°C). In winter, Zhengzhou again recorded the highest SUHII (1.67°C), followed by Xinxiang (1.38°C) and Xuchang (1.33°C), while the lowest intensity was recorded in Jiaozuo (0.71°C).

Among the four seasons, spring and summer recorded higher SUHIs in each city during the day. Among the examined cities, similarly to the results reported in Figure 1, Zhengzhou, Xuchang, and Xinxiang exhibited relatively high SUHIs, while the values in Kaifeng and Jiaozuo were low.

3.2 Temporal variation of daytime and nighttime SUHIs

3.2.1 Interannual variation of daytime and nighttime SUHIs

The annual average daytime and nighttime SUHIs in each city from 2003 to 2022 were plotted to determine temporal variations, and the results are shown in Figure 3. During the day, the SUHII in Kaifeng and Jiaozuo showed a fluctuating downward trend from 2003 to 2018, while that in Zhengzhou, Xuchang, and Xinxiang showed an increasing trend from 2003 to 2008 and a fluctuating downward trend from 2008 to 2018 (Figure 3A). After 2018, the overall trend in all cities except for Jiaozuo showed a significant increase. The daytime SUHII in Zhengzhou was positive in all years examined, while in the other cities it was positive in most years and negative in some years. Specifically, in Kaifeng, SUHII was negative in 2016, 2019, and 2022, with values of -0.04°C, -0.14°C, and -0.10°C, respectively. In Jiaozuo and Xinxiang, this parameter was negative in 2018, with values of -0.02°C and -0.38°C, respectively. In Xuchang, it was negative in 2013, with a value of -0.18°C.

In all cities except for Jiaozuo, SUHII showed a fluctuating upward trend at night. In 2003, the nighttime SUHIs in Kaifeng, Xinxiang, Xuchang, and Zhengzhou were 0.67°C, 0.87°C, 1.04°C, and 0.92°C, respectively. By 2022, these values had increased to 1.12°C, 0.98°C, 1.33°C, and 1.69°C, respectively.

The daytime and nighttime SUHIs in the study area in summer and winter from 2003 to 2022 were plotted to analyze temporal variations in different seasons. The temporal changes in SUHII during summer days reported in Figure 4 indicate no significant increasing or decreasing trends in the cities examined. Among these, Zhengzhou exhibited a relatively large fluctuation in SUHII values during summer days. However, during summer nights, the intensities generally increased in all cities, and the increase was significant especially between 2003 and 2010 (Figure 4B). During winter days, SUHII showed a decreasing trend in all cities before 2009 and displayed interannual non-significant fluctuations after 2009, which basically indicated the presence of the cold island effect (Figure 4C). During winter nights, SUHII did not vary significantly in Jiaozuo, but in the other cities it generally showed an increasing trend (Figure 4D).

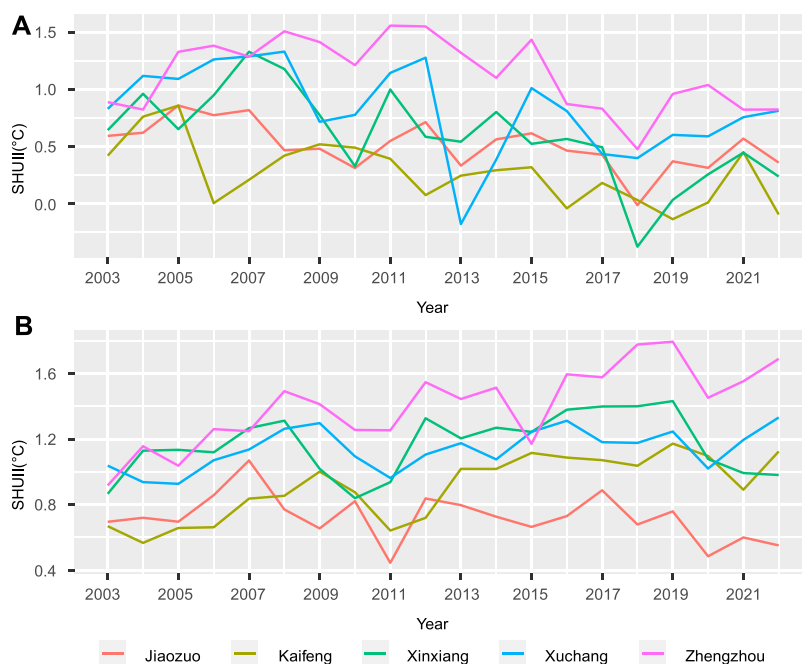


FIGURE 3 Temporal variation of surface heat island intensity in each city of the Zhengzhou metropolitan area between 2003 and 2022: (A) day, (B) night.

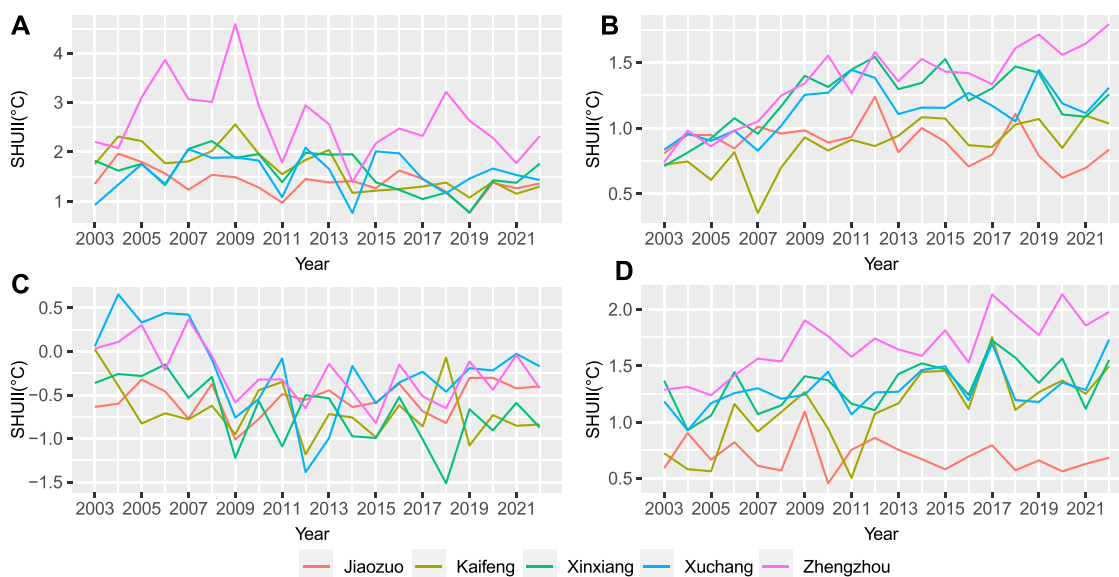


FIGURE 4 Temporal variation of SUHII in each city of the Zhengzhou metropolitan area during summer and winter from 2003 to 2022: (A) summer daytime, (B) summer nighttime, (C) winter daytime, (D) winter nighttime.

3.3 Variations and spatial differences in daytime and nighttime SUHIs within cities

SUHII was expected to vary at different locations within each city. The pixel-scale SUHII was here calculated based on the daytime and nighttime surface temperatures of urban and suburban areas in

each city from 2003 to 2022. Then, based on the values obtained for each year, the Sen’s slope was calculated at the pixel scale and the Mann–Kendall trend test was conducted. Using a confidence level of 95% ($\alpha = 0.05$, $Z = 1.96$), the SUHII trends of all cities were categorized into four types: significant increase, non-significant increase, significant decrease, and non-significant decrease.

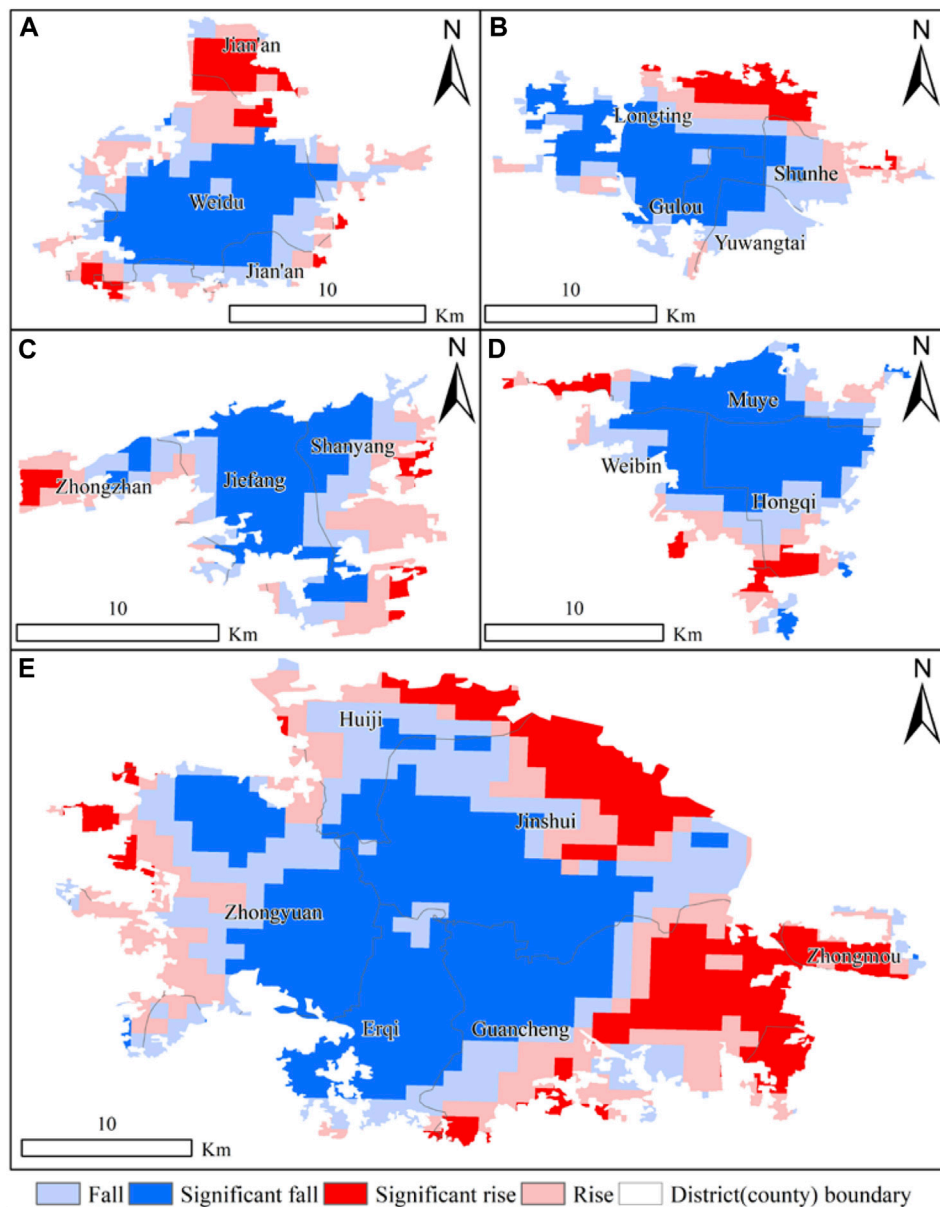


FIGURE 5 Spatial distribution of daytime SUHII trends in different cities within the Zhengzhou metropolitan area: (A) Xuchang, (B) Kaifeng, (C) Jiaozuo, (D) Xinxiang, (E) Zhengzhou.

Figure 5 shows the spatial distribution of daytime SUHII trends in the five cities examined. This parameter significantly decreased during the day in the old city areas and increased primarily in the peripheral urban areas, namely, in the northern parts of Xuchang (Figure 5A) and Kaifeng (Figure 5B), the eastern and western parts of Jiaozuo (Figure 5C), the western and southern parts of Xinxiang (Figure 5D), and the northeastern and southeastern parts of Zhengzhou (Figure 5E). The proportion of areas showing a significant decrease in SUHII during the daytime was relatively large in each city (Table 2). Specifically, the proportion in the urban area of Xinxiang was the largest, at 55.11%, while that in the urban area of Zhengzhou was the smallest, but still up to 39.67%. The areas in each city showing a significant increase in SUHII during the

daytime were relatively small. The largest proportion (18.02%) was detected in the urban area of Zhengzhou, followed by Xuchang (12.04%) and Kaifeng (10.44%). In both the urban areas of Xinxiang and Jiaozuo, the proportion was lower than 7.00%.

Figure 6 shows the spatial distribution of nighttime SUHII trends for the five cities examined. A significant decrease in nighttime SUHII was detected southwest of Xuchang (Figure 6A), while a significant increase was observed northeast of this city. In other areas, the upward or downward trends were not significant. In Kaifeng, most areas northwest of Longting District showed a significant increase in SUHII at night, while other areas mainly exhibited non-significant upward or downward trends (Figure 6B). In the southern part of Jiaozuo, the nighttime SUHII

TABLE 2 Proportion of areas (%) showing increasing (Rise) or decreasing (Fall) trends in SUHII during the day and at night in different cities within the Zhengzhou metropolitan area.

City	Day				Night			
	Fall	Fall*	Rise*	Rise	Fall	Fall*	Rise*	Rise
Jiaozuo	26.24	43.05	5.08	25.62	36.27	35.86	13.93	13.93
Kaifeng	31.10	43.96	10.44	14.50	27.61	6.18	41.15	25.07
Xinxiang	25.24	55.11	6.92	12.73	29.63	4.65	14.70	51.02
Xuchang	25.39	40.25	12.04	22.32	31.98	10.11	28.38	29.54
Zhengzhou	23.58	39.67	18.02	18.73	16.43	4.66	51.51	27.41

Note: *represents significant values.

increased significantly, while in some central, northeastern, and northwestern areas of the city, this parameter showed a significant decrease (Figure 6C). Significant increases in nighttime SUHII were observed in some eastern, southeastern, and northern areas of Xinxiang (Figure 6D), while some small areas northwest and southwest of this city showed significant decreases in this parameter. In most other areas, the upward or downward trends were not significant. Significant increases in nighttime SUHII were observed in most southeastern, northwestern, and southwestern areas of Zhengzhou (Figure 6E), while individual areas northeast and southwest of this city showed a significant decrease in this parameter. The values in the old city area and its surroundings exhibited a downward and upward trend, respectively, but these were not significant.

Based on the data reported in Table 2, large areas of Kaifeng (51.51%) and Zhengzhou (41.14%) exhibited a significant increase in nighttime SUHII, while this trend was observed in relatively small areas in Jiaozuo (13.93%) and Xinxiang (14.70%). The largest area showing a significant decrease in nighttime SUHII was detected in Jiaozuo, reaching 35.86%, followed by Xuchang at 10.11%. In all the other cities, the proportions were smaller than 6.50%.

Several studies have been conducted to investigate urban heat island in the study area. However, previous research has primarily focused on Zhengzhou. Notably, Min et al. (2018) and Yang et al. (2022) examined the temporal and spatial variations of urban heat island using radiation brightness temperature data for the periods of 1996–2014 and 2006–2020, respectively (Min et al., 2018; Yang Y. et al., 2022). These studies analyzed the spatial patterns of urban heat island and documented the area of urban heat island generally increased during over the study periods. Additionally, Min et al. (2018) reported an overall rise in average land surface temperature during 1996–2014. Furthermore, Zhou et al. (2022) investigated the temporal and spatial variations of land surface temperature across the entire city of Zhengzhou, encompassing both urban and rural areas (Zhou et al., 2022). The study utilized the MODIS land surface temperature data from 2005 to 2020 and found that the average land surface temperature exhibited an upward trend, with the urban heat island predominantly concentrated in the main city. It is important to note that these aforementioned studies differ significantly from the present study, as they used land surface temperature as a metric to characterize urban heat island and focused on analyzing the spatial distribution and temporal changes of land surface temperature. Nevertheless, there were some similar findings

indicating a general increasing trend in surface temperature within Zhengzhou (see Fig. A1 and Fig. A2).

4 Discussion

In this study, the SUHII in the cities of the Zhengzhou metropolitan area was calculated and its temporal variation, seasonal differences, and spatial differences during the day and at night were analyzed. The core city of the metropolitan area, Zhengzhou, exhibited the strongest SUHII and, in all cities examined, this parameter was higher during the day than at night. Significant seasonal differences in SUHII were detected in each city, with generally stronger daytime intensities in summer and cold island effects in winter. From 2003 to 2022, the annual average SUHII at night and the average SUHII in summer and winter nights showed overall increasing trends in all cities except for Jiaozuo. Values varied significantly in different areas within each city during the day, with significant downward trends detected in the central areas (referred to as “old city”) and significant upward trends in some peripheral areas. Significant regional differences in the increase or decrease of nighttime SUHII in each city were also observed.

The urban heat island effect is a widespread phenomenon, especially in large cities (Yang et al., 2019), and the present study confirmed that the city of Zhengzhou had the strongest SUHII in the metropolitan area. In comparison, the values detected in Kaifeng and Jiaozuo were relatively low, and this difference is closely related to the geographical environment of these two cities. Kaifeng, known as the “water city” of northern China, has many water bodies in its urban area, which result in a weak heat island effect. Due to the exposure of Jiaozuo to the Taihang Mountain in the north and its winds, the nighttime surface temperature in this city was lower than 1°C, and SUHII was also consequently low. As reported in previous studies of the seasonal patterns of SUHII in Chinese cities (Zhou et al., 2014; Wang et al., 2015), the present study found that the daytime heat island effect in the Zhengzhou metropolitan area was the strongest in summer, followed by that in spring, autumn, and winter, while the nighttime heat island effect was stronger in spring and winter and weaker in summer and autumn. The Zhengzhou metropolitan area is located in the temperate monsoon climate zone of the northern hemisphere and is characterized by long sunshine hours and a high solar elevation angle in summer. The continuous heat storage by artificial surfaces in urban areas causes

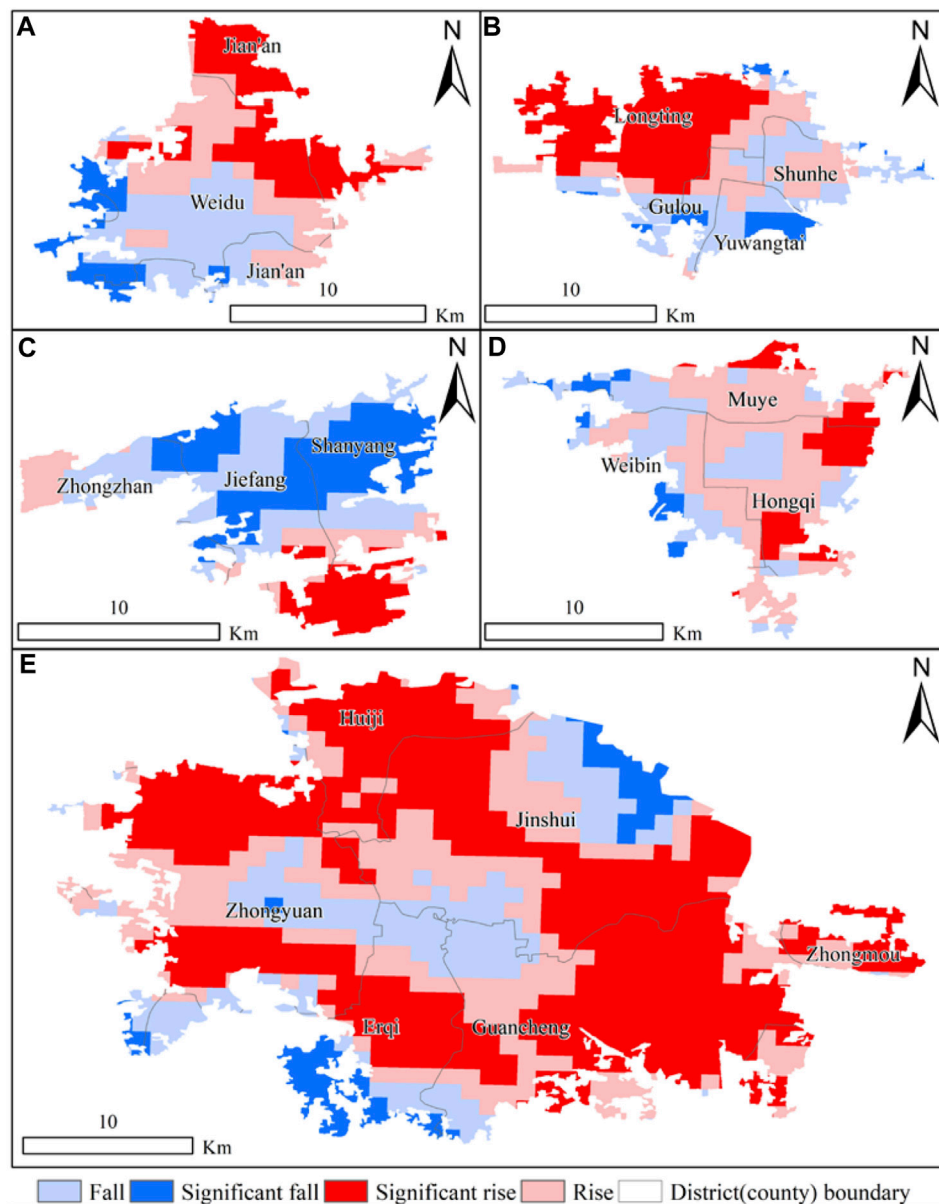


FIGURE 6

Spatial distribution of nighttime SUHII trends in different cities within the Zhengzhou metropolitan area: (A) Xuchang, (B) Kaifeng, (C) Jiaozuo, (D) Xinxiang, (E) Zhengzhou.

higher daytime surface temperatures that result in stronger daytime SUHII in summer. In contrast, in suburban areas, where there are more agricultural activities or forest vegetation, the evapotranspiration effect of plants reduces surface temperatures (Yao et al., 2019; Meng et al., 2023). In this study, the lowest SUHII were detected in winter, indicating the presence of the cold island effect, which is associated with weak solar radiation and differences in the thermal properties of urban and suburban areas. This effect has been shown to vary in different regions. At night, suburban vegetation activity and reduced surface reflectivity as well as human-induced heat emissions cause higher surface temperatures in urban areas than in suburban areas in all seasons (Yang et al., 2019).

In terms of the interannual variation of daytime and nighttime SUHII, we found no significant trends during the day in any of the cities examined, except for Jiaozuo. However, the SUHII at night showed an increasing trend in all cities except for Jiaozuo. In terms of seasonal variation, no clear trend in daytime SUHII was detected either in winter or summer. However, the nighttime SUHII in summer showed a clear increasing trend in all cities, while that in winter showed a clear increasing trend for all cities except for Jiaozuo. Similar findings have also been reported in other studies (Zhou et al., 2016; Meng et al., 2018). The present study also revealed the spatial differences in SUHII within urban areas. During the day, this parameter exhibited a significant decreasing trend in the “old city” areas and a non-

significant decreasing trend in the surrounding areas. On the other hand, some areas on the outskirts of the cities examined showed a significant increasing trend. This indicated that the urban heat islands effect shifts from central cities to the suburbs, and we believe that this phenomenon is related to the processes of urbanization and spatial expansion of cities. The earliest increases in surface temperature and SUHII were recorded in the central areas of cities, which were developed first. With the expansion of cities, the surface temperature in the peripheral areas increased rapidly, leading to an increase in surface temperature in the suburbs. At the same time, the surface temperature in the old cities increased relatively slowly due to the higher initial surface temperature. Consequently, the difference in the increase of surface temperature between the central and peripheral areas (see Figure A1) resulted in a weaker increase in SUHII in the central area, and even in a decreasing trend. At night, obvious differences among cities were detected in the areas where SUHII significantly increased or decreased. This was due to the main direction of urban expansion and to the population and industrial concentrations in each city. Over the past 20 years, Xuchang has mainly expanded to the northeast, Kaifeng has expanded on a large scale in Longting District, and Jiaozuo and Xuchang have expanded toward their southeastern/eastern areas. In contrast, in Zhengzhou, the areas of urban and population expansion have been the eastern Zhengdong New District, southeastern Economic Development Zone, northwestern High-Tech Zone, and Huiji District, and they have been rapidly developed moving from the city center toward the periphery.

The above findings can contribute to the understanding of the spatiotemporal dynamics of the urban heat island effect in the study area. Especially, the spatial differences in SUHII within urban areas, which previous studies have focused less on, were also revealed. The specific mechanisms that determine the urban heat island effect in each city and its influencing factors are different and complex and need to be further investigated. However, urbanization and urban expansion undoubtedly resulted in spatial differences in the increase of surface temperature (Figure A2) and SUHII within each city. In addition, the large area of the water body (in Kaifeng) effectively mitigates the urban heat island effect from the comparison of heat island effects in the five cities. Thus, these findings have important practical policy implications for the ongoing urban renewal projects and urbanization development planning in China. It is recommended to add more green vegetation around buildings, city roads, and large squares, and to include new water urban bodies, and increase the existing urban water bodies according to the area of urban function zones. The plan for ventilation corridors and green belts between urban function zones should be given full attention in future urbanization and urban agglomeration development.

There were two main aspects of limitation that needed clarification in this study. The first was the coarse resolution of the surface temperature data. A resolution of 1 km is sufficient to reveal spatial differences in surface temperatures at a regional or national scale, but it fails to capture the spatial variability in temperature within urban areas effectively. Fortunately, significant progress has been made in producing finer resolution surface temperature data products, such as 100 m and 30 m, based on the Landsat data (Wang et al., 2020; Cheng et al., 2021). Therefore, finer-resolution surface temperature product data should be

applied in future studies. The second limitation stems from the division of urban areas and suburban areas. Urban areas are dynamic and rapidly expand into rural regions. In urban agglomerations, some cities are even adjacent to each other through critical infrastructure and functional zones, blurring the boundaries between urban and suburban areas. Consequently, some urban areas may be excluded in this study. More scientific and effective quantization methods for defining urban and suburban areas should be explored, particularly in urban agglomerations.

5 Conclusion

In this study, the SUHIIs of cities in the Zhengzhou metropolitan area were calculated based on the difference in surface temperature between urban and suburban areas. Then, the differences in this parameter during the day and at night, as well as its seasonal variation, temporal trends, and spatial differences among different cities were analyzed. Overall, it was shown that Zhengzhou, the core city of the metropolitan area, had the strongest urban heat island effect. The nighttime SUHII of each city examined exhibited a clear increasing trend; however, the daytime SUHIIs outside the urban areas showed a significant decreasing trend, while the nighttime values in the main regions of urban expansion in each city showed a clear increasing trend. The results obtained provided a knowledge base to understand the spatiotemporal variation of the urban heat island effect in the Zhengzhou metropolitan area.

Data availability statement

The original contributions presented in the study are included in the article/Supplementary Material, further inquiries can be directed to the corresponding author.

Author contributions

GT conceived and designed the study. FM initiated the study and undertook statistical analysis and manuscript writing. FM undertook data curation and revised the manuscript. YW designed the methodology. SY provided useful suggestions. All authors contributed to the article and approved the submitted version.

Funding

This study was sponsored by the Key Scientific and Technological Project of Henan Province, China (Grant No. 222400410101).

Conflict of interest

The authors declare that the research was conducted in the absence of any commercial or financial relationships that could be construed as a potential conflict of interest.

Publisher's note

All claims expressed in this article are solely those of the authors and do not necessarily represent those of their affiliated

organizations, or those of the publisher, the editors and the reviewers. Any product that may be evaluated in this article, or claim that may be made by its manufacturer, is not guaranteed or endorsed by the publisher.

References

- Chen, M., Liu, W., Lu, D., Chen, H., and Ye, C. Progress of China's new-type urbanization construction since 2014: A preliminary assessment. *Cities* 2018, 78, 180–193. doi:10.1016/j.cities.2018.02.012
- Cheng, Jie., Meng, X., Dong, S., and Liang, S. Generating the 30-m land surface temperature product over continental China and USA from landsat 5/7/8 data. *Sci. Remote Sens.* 2021, 4: 100032. doi:10.1016/j.srs.2021.100032
- Clinton, N., and Gong, P. MODIS detected surface urban heat islands and sinks: Global locations and controls. *Remote Sens. Environ.* 2013, 134, 294–304. doi:10.1016/j.rse.2013.03.008
- Debbage, N., and Shepherd, J. M. The urban heat island effect and city contiguity. *Comput. Environ. Urban Syst.* 2015, 54, 181–194. doi:10.1016/j.compenvurbsys.2015.08.002
- Deilami, K., Kamruzzaman, M., and Liu, Y. Urban heat island effect: A systematic review of spatio-temporal factors, data, methods, and mitigation measures. *Int. J. Appl. Earth Obs. Geoinf.* 2018, 67, 30–42. doi:10.1016/j.jag.2017.12.009
- Halder, B., Bandyopadhyay, J., and Banik, P. Evaluation of the climate change impact on urban heat island based on land surface temperature and geospatial indicators. *Int. J. Environ. Res.* 2021, 15, 819–835. doi:10.1007/s41742-021-00356-8
- Henan Province Bureau of Statistics. 2022 *Henan statistical yearbook*. Beijing, China: China Statistics Press.
- Ke, X., Men, H., Zhou, T., Li, Z., and Zhu, F. Variance of the impact of urban green space on the urban heat island effect among different urban functional zones: A case study in wuhan. *Urban For. Urban Green.* 2021, 62, 127159. doi:10.1016/j.ufug.2021.127159
- Khan, A., and Chatterjee, S. Numerical simulation of urban heat island intensity under urban-suburban surface and reference site in Kolkata, India. *Earth Syst. Environ.* 2016, 2, 71. doi:10.1007/s40808-016-0119-5
- Kumar, R., and Mishra, V. Decline in surface urban heat island intensity in India during heatwaves. *Environ. Res. Commun.* 2019, 1, 031001. doi:10.1088/2515-7620/ab121d
- Levermore, G., Parkinson, J., Lee, K., Laycock, P., and Lindley, S. The increasing trend of the urban heat island intensity. *Urban Clim.* 2018, 24, 360–368. doi:10.1016/j.uclim.2017.02.004
- Li, Y., Schubert, S., Kropp, J. P., and Rybski, D. On the influence of density and morphology on the urban heat island intensity. *Nat. Commun.* 2020, 11, 2647. doi:10.1038/s41467-020-16461-9
- Liao, W., Cai, Z., Feng, Ye., Gan, D., and Li, X. A simple and easy method to quantify the cool island intensity of urban greenspace. *Urban For. Urban Green.* 2021, 62: 127173. doi:10.1016/j.ufug.2021.127173
- Liu, X., Zhou, Y., Yue, W., Li, X., Liu, Y., and Lu, D. Spatiotemporal patterns of summer urban heat island in Beijing, China using an improved land surface temperature. *J. Clean. Prod.* 2020b, 257, 120529. doi:10.1016/j.jclepro.2020.120529
- Liu, Y., Li, Q., Yang, L., Mu, K., Zhang, M., and Liu, J. Urban heat island effects of various urban morphologies under regional climate conditions. *Sci. Total Environ.* 2020a, 743, 140589. doi:10.1016/j.scitotenv.2020.140589
- Ma, J., Dong, G., Yao, B., Giannousis, P., Thoolen, M., Ye, Q., et al. Periodicity and variability in daily activity satisfaction: Toward a space-time modeling of subjective well-being. *Ann. Am. Assoc. Geogr.* 2023, 1, 1–19. doi:10.1080/00498254.2023.2245459
- Manoli, G., Faticchi, S., Schläpfer, M., Yu, K., Crowther, T. W., Meili, N., et al. Magnitude of urban heat islands largely explained by climate and population. *Nature* 2019, 573, 55–60. doi:10.1038/s41586-019-1512-9
- Marando, F., Heris, M. P., Zulian, G., Udías, A., Mentaschi, L., Chrysoulakis, N., et al. Urban heat island mitigation by green infrastructure in European functional urban areas. *Sustain. Cities Soc.* 2022, 77, 103564. doi:10.1016/j.scs.2021.103564
- Meng, Q., Zhang, L., Sun, Z., Meng, F., Wang, L., and Sun, Y. Characterizing spatial and temporal trends of surface urban heat island effect in an urban main built-up area: A 12-year case study in Beijing, China. *Remote Sens. Environ.* 2018, 204, 826–837. doi:10.1016/j.rse.2017.09.019
- Meng, X., Pi, H., Gao, X., He, P., and Lei, J. A high-accuracy vegetation restoration potential mapping model integrating similar habitat and machine learning. *L. Degrad. Dev.* 2023, 34, 1208–1224. doi:10.1002/ldr.4527
- Min, M., Zhao, H., and Miao, C. Spatio-temporal evolution analysis of the urban heat island: A case study of Zhengzhou city, China. *Sustainability* 2018, 10, 1992; doi:10.3390/su10061992
- Peng, S., Piao, S., Ciais, P., Friedlingstein, P., Ottle, C., Bréon, F.-M., et al. Surface urban heat island across 419 global big cities. *Environ. Sci. Technol.* 2012, 46, 696–703. doi:10.1021/es2030438
- Schwarz, N., Lautenbach, S., and Seppelt, R. Exploring indicators for quantifying surface urban heat islands of European cities with MODIS land surface temperatures. *Remote Sens. Environ.* 2011, 115, 3175–3186. doi:10.1016/j.rse.2011.07.003
- Sekertekin, A., and Zadbagher, E. Simulation of future land surface temperature distribution and evaluating surface urban heat island based on impervious surface area. *Ecol. Indic.* 2021, 122, 107230. doi:10.1016/j.ecolind.2020.107230
- Siddiqui, A., Kushwaha, G., Nikam, B., Srivastav, S. K., Shelar, A., and Kumar, P. Analysing the day/night seasonal and annual changes and trends in land surface temperature and surface urban heat island intensity (SUHI) for Indian cities. *Sustain. Cities Soc.* 2021, 75:103374. doi:10.1016/j.scs.2021.103374
- Sun, Z., Li, Z., and Zhong, J. Analysis of the impact of landscape patterns on urban heat islands: A case study of Chengdu, China. *Int. J. Environ. Res. Public Health* 2022, 19, 13297. doi:10.3390/ijerph192013297
- Tan, M., and Li, X. Quantifying the effects of settlement size on urban heat islands in fairly uniform geographic areas. *Habitat Int.* 2015, 49, 100–106. doi:10.1016/j.habitatint.2015.05.013
- Tong, S., Prior, J., McGregor, G., Shi, X., and Kinney, P. Urban heat: An increasing threat to global health. *BMJ* 2021, 375, n2467. doi:10.1136/bmj.n2467
- Vinayak, B., Lee, H. S., Gedam, S., and Latha, R. Impacts of future urbanization on urban microclimate and thermal comfort over the Mumbai metropolitan region, India. *Sustain. Cities Soc.* 2022, 79, 103703. doi:10.1016/j.scs.2022.103703
- Wang, J., Chen, Y., Liao, W., He, G., Tett, S. F. B., Yan, Z., et al. Anthropogenic emissions and urbanization increase risk of compound hot extremes in cities. *Nat. Clim. Chang.* 2021a, 11, 1084–1089. doi:10.1038/s41558-021-01196-2
- Wang, J., Huang, B., Fu, D., and Atkinson, P. M. Spatiotemporal variation in surface urban heat island intensity and associated determinants across major Chinese cities. *Remote Sens.* 2015, 7, 3670–3689. doi:10.3390/rs70403670
- Wang, M., Zhang, Z., Hu, T., Wang, G., He, G., Zhang, Z., et al. An efficient framework for producing landsat-based land surface temperature data using Google Earth engine. *IEEE J. Sel. Top. Appl. Earth Observations Remote Sens.* 2020, 13: 4689–4701. doi:10.1109/JSTARS.2020.3014586
- Wang, X., Tian, G., Yang, D., Zhang, W., Lu, D., and Liu, Z. Responses of PM_{2.5} pollution to urbanization in China. *Energy Policy* 2018, 123, 602–610. doi:10.1016/j.enpol.2018.09.001
- Wang, Y., Guo, Z., and Han, J. The relationship between urban heat island and air pollutants and them with influencing factors in the Yangtze River Delta, China. *Ecol. Indic.* 2021b, 129: 107976. doi:10.1016/j.ecolind.2021.107976
- Wu, X., Wang, G., Yao, R., Wang, L., Yu, D., and Gui, X. Investigating surface urban heat islands in South America based on MODIS data from 2003–2016. *Remote Sens.* 2019, 11, 1212. doi:10.3390/rs11101212
- Yang, D., Meng, F., Liu, Y., Dong, G., and Lu, D. Scale effects and regional disparities of land use in influencing pm 2.5 concentrations: A case study in the Zhengzhou metropolitan area, China. *Land* 2022a, 11, 1538. doi:10.3390/land11091538
- Yang, F., Li, S., Gao, Y., Li, M., and Wu, P. Inconsistent carbon budget estimation using dynamic/static carbon density under land use and land cover change: A case study in henan Province, China. *Land* 2022b, 11, 2232. doi:10.3390/land11122232
- Yang, Q., Huang, X., and Tang, Q. The footprint of urban heat island effect in 302 Chinese cities: Temporal trends and associated factors. *Sci. Total Environ.* 2019, 655, 652–662. doi:10.1016/j.scitotenv.2018.11.171
- Yang, Y., Song, F., Ma, J., Wei, Z., Song, L., and Cao, W. Spatial and temporal variation of heat islands in the main urban area of Zhengzhou under the two-way influence of urbanization and urban forestry. *PLoS ONE* 2022c, 17(8): e0272626. doi:10.1371/journal.pone.0272626
- Yao, R., Wang, L., Huang, X., Gong, W., and Xia, X. Greening in rural areas increases the surface urban heat island intensity. *Geophys. Res. Lett.* 2019, 46, 2204–2212. doi:10.1029/2018GL081816

Zhang, H., Yin, Y., An, H., Lei, J., Li, M., Song, J., et al. Surface urban heat island and its relationship with land cover change in five urban agglomerations in China based on GEE. *Environ. Sci. Pollut. Res.* 2022b, 29: 82271–82285. doi:10.1007/s11356-022-21452-y

Zhang, X., Chen, L., Jiang, W., and Jin, X. Urban heat island of Yangtze River Delta urban agglomeration in China: Multi-time scale characteristics and influencing factors. *Urban Clim.* 2022a, 43, 101180, doi:10.1016/j.uclim.2022.101180

Zhao, M., Cai, H., Qiao, Z., and Xu, X. Influence of urban expansion on the urban heat island effect in shanghai. *Int. J. Geogr. Inf. Sci.* 2016, 30, 2421–2441. doi:10.1080/13658816.2016.1178389

Zhou, D., Zhang, L., Hao, L., Sun, G., Liu, Y., and Zhu, C. Spatiotemporal trends of urban heat island effect along the urban development intensity gradient in China. *Sci. Total Environ.* 2016, 544, 617–626. doi:10.1016/j.scitotenv.2015.11.168

Zhou, D., Zhao, S., Liu, S., Zhang, L., and Zhu, C. Surface urban heat island in China's 32 major cities: Spatial patterns and drivers. *Remote Sens. Environ.* 2014, 152, 51–61. doi:10.1016/j.rse.2014.05.017

Zhou, S., Liu, D., Zhu, M., Tang, W., Chi, Q., Ye, S., et al. Temporal and spatial variation of land surface temperature and its driving factors in Zhengzhou city in China from 2005 to 2020. *Remote Sens.* 2022, 14, 4281. doi:10.3390/rs14174281

Appendix

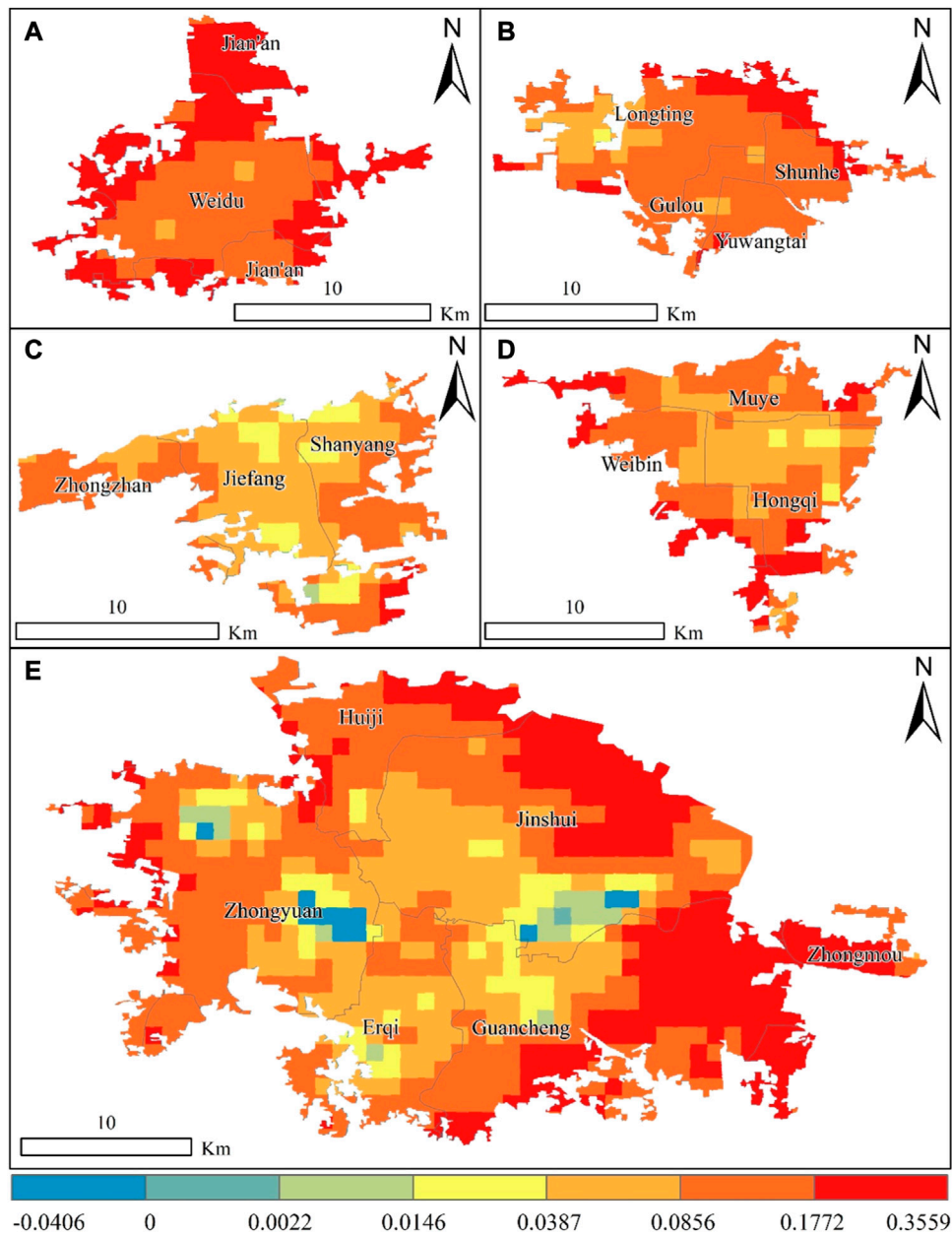


FIGURE A1
Spatial distribution of daytime surface temperature trends in different cities within the Zhengzhou metropolitan area.

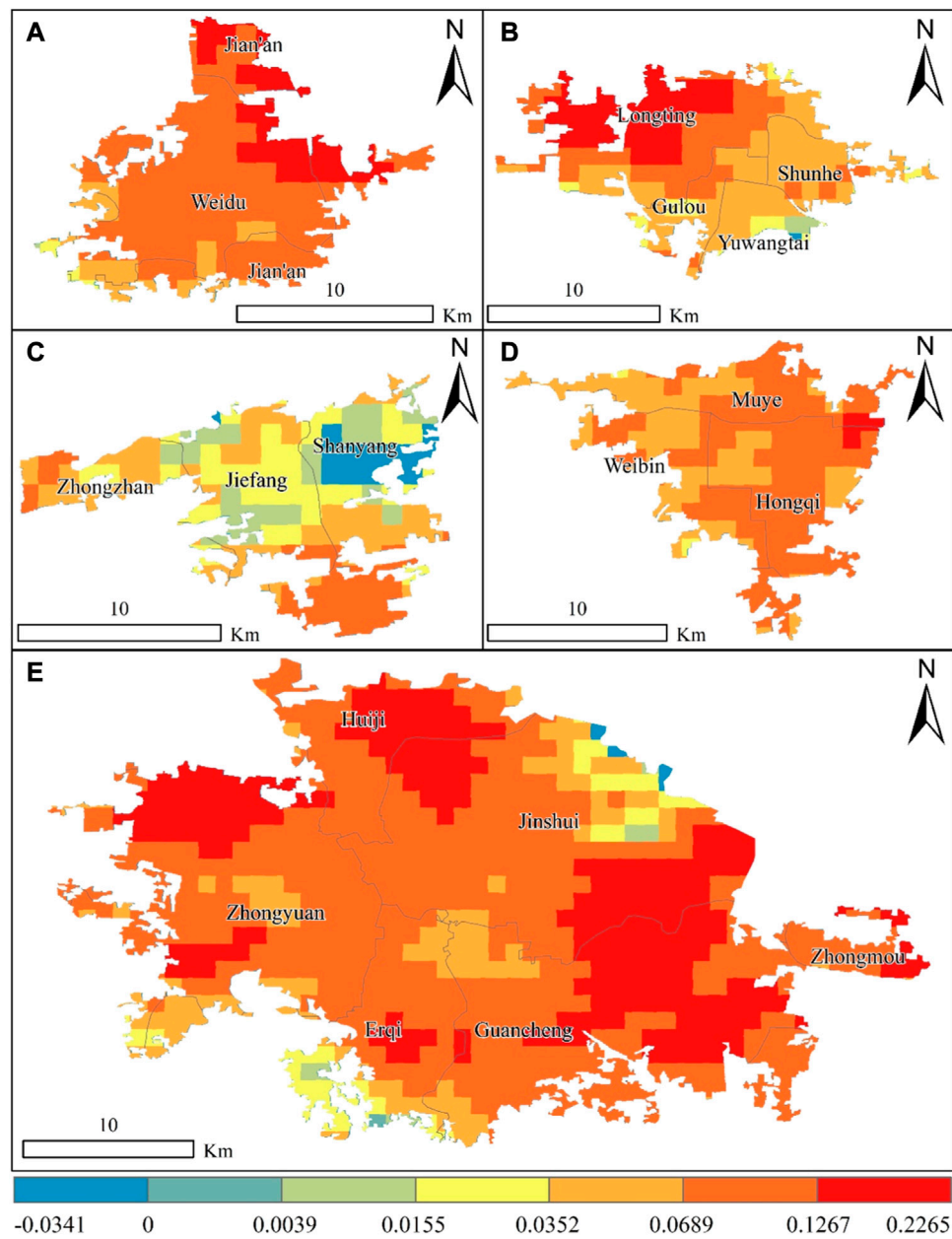


FIGURE A2
Spatial distribution of nighttime surface temperature trends in different cities within the Zhengzhou metropolitan area.